

Rotational spectroscopy of the thioformaldehyde isotopologues H_2CS and $\text{H}_2\text{C}^{34}\text{S}$ in four interacting excited vibrational states and an account on the rotational spectrum of thioketene, H_2CCS

Holger S. P. Müller^a, Atsuko Maeda^b, Frank Lewen^a, Stephan Schlemmer^a, Ivan R. Medvedev^{b,c} and Eric Herbst^{b,d}

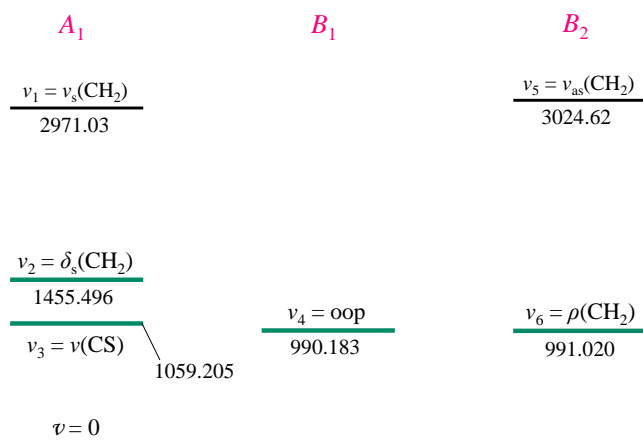
^aAstrophysik/I. Physikalisches Institut, Universität zu Köln, Zùlpicher Str. 77, 50937 Köln, Germany; ^bDepartment of Physics, The Ohio State University, Columbus, OH 43210-1107, USA; ^cDepartment of Physics, Wright State University, Dayton, OH 45435, USA; ^dDepartments of Chemistry and Astronomy, University of Virginia, Charlottesville, VA 22904, USA

ARTICLE HISTORY

Compiled September 26, 2023

ABSTRACT

An investigation of the rotational spectrum of the interstellar molecule thioformaldehyde between 110 and 377 GHz through a pyrolysis reaction revealed a multitude of absorption lines assignable to H_2CS and $\text{H}_2\text{C}^{34}\text{S}$ in their lowest four excited vibrational states besides lines of numerous thioformaldehyde isotopologues in their ground vibrational states reported earlier as well as lines pertaining to several by-products. Additional transitions of H_2CS in its lowest four excited vibrational states were recorded in selected regions between 571 and 1386 GHz. Slight to strong Coriolis interactions occur between all four vibrational states with the exception of the two highest lying states because both are totally symmetric vibrations. We present combined analyses of the ground and the four interacting states for our rotational data of H_2CS and $\text{H}_2\text{C}^{34}\text{S}$. The H_2CS data were supplemented with two sets of high-resolution IR data in two separate analyses. The $v_2 = 1$ state has been included in analyses of Coriolis interactions of low-lying fundamental states of H_2CS for the first time and this improved the quality of the fits substantially. We extended furthermore assignments in J of transition frequencies of thioketene in its ground vibrational state.



KEYWORDS

Rotational spectroscopy; excited vibrational states; rotation-vibration interaction; interstellar molecule

CONTACT Holger S. P. Müller. Email: hspm@ph1.uni-koeln.de

Supplemental data for this article can be accessed at <https://doi.org/10.1080/...>

1. Introduction

Thioformaldehyde, H₂CS, is as a small molecule of C_{2v} symmetry obviously of fundamental interest in particular in comparison to its lighter sibling formaldehyde, H₂CO. Its rotational spectrum received additional attention because it served as a mean to identify the molecule in a variety of astronomical sources. It was detected first in the giant high-mass starforming region Sagittarius B2 near the Galactic centre [1] and later in dark clouds [2], circumstellar envelopes of late-type stars [3], nearby [4, 5] and more distant galaxies [6] and also in the comet Hale–Bopp [7]. Several of its isotopologues were also found in space, including H₂C³⁴S [8], H₂¹³C³⁴S [9], HDCS [10] and D₂CS [11], where unlabelled atoms refer to ¹²C and ³²S. Rotational transitions of thioformaldehyde were employed more recently to infer temperature in [12] or the structure of disks around young stellar objects [13] or to investigate deuteration in a prestellar core [14].

The first report on the rotational spectrum of the main isotopologue was published in 1970 [15]. Later studies extended the frequency range to 245 GHz or presented data on isotopic species [16–19]. Transition frequencies of HDCS were determined some time later [10], and astronomical observations were employed to improve mainly the D₂CS data set [11]. The dipole moment of H₂CS was determined through Stark effect measurements [16, 20]. All these studies were restricted to the ground vibrational states.

Medium- and high-resolution IR investigations were performed in the CH₂ stretching region covering ν_5 , ν_1 and $2\nu_2$ [21], in the ν_2 CH₂ bending region [22] and around 10 μm [23–25]. The 10 μm studies include laser Stark spectroscopy of ν_4 , ν_6 and ν_3 with determination of permanent dipole moments in the excited vibrational states [23], an FTIR investigation of ν_4 and ν_6 of H₂CS with additional results on D₂CS, a harmonic force field calculation and an estimate of the equilibrium structure of thioformaldehyde [24] and finally an extensive FTIR study of ν_4 , ν_6 and ν_3 [25].

Thioformaldehyde has also been subjected to several studies of its electronic spectrum. Most of these were, however, of limited impact for the data in the ground electronic state. A notable exception is a sub-Doppler spectroscopic investigation of a part of the $\tilde{A} - \tilde{X}$ spectrum that yielded ground state combination differences which improved the purely K -depended parameters considerably [26].

There have also been numerous quantum-chemical calculations on structural or vibrational properties of H₂CS, in particular in the past 30 years [27–32]. The existing experimental rotational and rovibrational data were evaluated recently [33], and the results were employed in a refinement of a quantum-chemically generated potential energy surface to generate a high-temperature line list of H₂CS [34]. We mention furthermore calculations of the properties of isomers of thioformaldehyde [35, 36]. Finally, H₂CS served also as an example to improve [37] or develop programs to calculate line intensities [38] or spectroscopic parameters [39].

Large uncertainties in the transition frequencies of the H₂CS main isotopologue in the sub-millimetre region prompted us to investigate the rotational spectrum of thioformaldehyde at The Ohio State University and subsequently at the Universität zu Köln resulting in a report on the main isotopic species [40]. Measurements at the Universität zu Köln were extended in frequency some time later leading to a further improved account on the spectra of the main isotopologue and data pertaining to several minor isotopic species observed in natural isotopic composition, including the very rare H₂¹³C³⁴S, HDCS and H₂C³⁶S [32]. The wealth of accurate rotational parameters of many isotopic species was taken to evaluate a semi-empirical equilibrium structure with vibration–rotation parameters from quantum-chemical calculations [32]. The measurements carried out at The Ohio State University covered large sections of the millimetre wave and the lower part of the submillimetre wave region continuously and revealed many more absorption features besides those of several thioformaldehyde isotopologues in their ground vibrational states. A large amount of these lines could be assigned to transitions of H₂CS and H₂C³⁴S in their lowest four excited vibrational states. Other lines could be assigned to by-products of the pyrolysis reaction through which thioformaldehyde was generated. Our present and final work on the rotational spectroscopy of thioformaldehyde deals with analyses

of the Coriolis-coupled lowest four excited vibrational states of H_2CS and $\text{H}_2\text{C}^{34}\text{S}$. These states are in fact textbook examples of Coriolis coupling because $v_4 = 1$ and $v_6 = 1$ are essentially degenerate, $v_3 = 1$ is quite close to these two states while $v_2 = 1$ is more distant, but still close enough that it is necessary to consider this state in the analyses. We supplement our H_2CS analyses by two sets of high-resolution data of ν_4 , ν_6 and ν_3 and one set of data of ν_2 . We present also a reanalysis of the ground state rotational spectrum of thioketene, $\text{H}_2\text{C}_2\text{S}$, one of the by-products of the pyrolysis reaction, whose rotational spectrum was presented up to 226 GHz in the previous literature [41–43]. It is worthwhile mentioning that its ground state spectroscopic parameters were also improved in a far- and mid-IR spectroscopic study [44] and that it was detected in the cold and dense prestellar core TMC-1 quite recently besides several other sulfur-containing molecules [45].

The rest of this manuscript is organised as follows. Section 2 provides details on our laboratory measurements. The spectroscopic properties of thioformaldehyde are described in Section 3 while Section 4 deals with considerations for the analyses and the fitting of the spectra. Our results are detailed in Section 5, discussed in Section 6 and concluding remarks are presented in Section 7.

2. Laboratory spectroscopic details

The Fast Scan Submillimetre-wave Spectroscopic Technique (FASSST) was developed at The Ohio State University (OSU) and employed there to cover most of the 110–377 GHz range [46–48]. We used furthermore two different spectrometer systems at the Universität zu Köln to record higher frequency transitions up to almost 1.4 THz [49–51].

The FASSST system applies backward wave oscillators (BWOs) as sources; in the present investigation one that covers about 110–190 GHz and two additional ones spanning the region of 200–377 GHz. The frequency of each BWO is swept very quickly such that a wide frequency range (~ 90 GHz) can be measured in a short period and any voltage instability of the BWOs can be overcome. Each FASSST spectrum requires calibration which was achieved through rotational lines of SO_2 . It displays sufficiently many spectral frequencies which are well known [52]. A portion of the source radiation propagates through a Fabry–Perot cavity to produce an interference fringe spectrum with a free spectral range of ~ 9.2 MHz. The frequencies of radiation between the calibration lines are interpolated with the fringe spectrum. It is important to take the dispersive effect of atmospheric water vapour in the Fabry–Perot cavity into account in the calibration procedure [53, 54]. Measurements were taken with scans that proceeded both upward and downward in frequency to record an average frequency. The results obtained from 100 upward and downward scans were accumulated for a better signal-to-noise ratio (S/N), increasing the integration time from ~ 0.1 to ~ 10 ms per Doppler limited line width. The experimental uncertainty of this apparatus is around 50 kHz for an isolated, well-calibrated line.

The Cologne spectrometers are equipped with phase-lock loop (PLL) systems to obtain accurate frequencies. Two BWOs were employed as sources to record usually individual lines in the 566–670 and 848–930 GHz regions. A portion of the radiation from the BWOs is mixed with an appropriate harmonic of a continuously tunable synthesiser in a Schottky diode multiplier mixer to produce the intermediate frequency (IF) signal. The IF signal is phase locked and the phase error provided by the PLL circuit is fed back to the power supply of the BWOs. Further details on this spectrometer system are available elsewhere [49, 50].

Virginia Diode Inc. (VDI) frequency multipliers driven by an Agilent E8257D microwave synthesiser were used to record transition frequencies between 1290 and 1390 GHz [51]. Both spectrometer systems achieve accuracies of 10 kHz and even better for very symmetric lines with good S/N as shown in recent studies on vibrationally excited methyl cyanide [55] or on isotopic oxirane [56].

Thioformaldehyde (H_2CS) was generated by the pyrolysis of trimethylene sulfide [$(\text{CH}_2)_3\text{S}$; Sigma-Aldrich Co.], which was used as provided. The thermal decomposition of trimethylene

sulfide affords thioformaldehyde and ethylene in high yields. Ethylene does not have a permanent dipole moment so its presence is essentially negligible. Small amounts of other by-products are present in the spectrum and include CS, H₂S and H₂CCS. Laboratory setups for the pyrolysis were slightly different in the OSU and Cologne measurements. At OSU, trimethylene sulfide vapour was passed through a 2-cm diameter, 20 cm long piece of quartz tubing stuffed with quartz pieces and quartz cotton to enlarge the reaction surface. The quartz tubing was heated with a cylindrical furnace to $\sim 680^\circ\text{C}$. The gas produced from the pyrolysis was introduced to a 6-m-long aluminum cell at room temperature and pumped to a pressure of 0.4–1.5 mTorr (1 mTorr = 0.1333 Pa). The spectrum of trimethylene sulfide disappeared almost totally after the pyrolysis, at which time the spectrum of thioformaldehyde appeared. Spectral lines of by-products were usually less intense compared with those of thioformaldehyde.

A 3-m-long glass absorption cell kept at room temperature was used for measurements at Cologne. A higher temperature of about 1300°C was required in the pyrolysis zone in order to maximise the thioformaldehyde yield and to minimise absorptions of (CH₂)₃S because no quartz cotton was used in the quartz pyrolysis tube. The total pressure was around 1–3 Pa for weaker lines and around 0.01–0.1 Pa for stronger lines.

Liquid He-cooled InSb bolometers were used in both laboratories as detectors. Frequency modulation was employed at Cologne to reduce baseline effects. The demodulation at twice the modulation frequency causes absorption lines to appear approximately as second derivatives of a Gaussian. Spectral baselines in OSU spectra were reduced by filtering of detector signals produced by fast scan of the radiation source through the spectral line. The detected effective line shape is near first derivative. Numerical differentiation leads to near second derivative line shapes. Additional digital filtering suppresses the baseline further.

3. Spectroscopic properties of thioformaldehyde

Thioformaldehyde is an asymmetric rotor with $\kappa = (2B - A - C)/(A - C) = -0.9924$ very close to the symmetric limit of -1 . Its dipole moment of 1.6491 D [20] is aligned with the a inertial axis. The strong rotational transitions are therefore those with $\Delta K_a = 0$ and $\Delta J = +1$ called R -branch transitions. Transitions with $\Delta K_a = 0$ and $\Delta J = 0$ (Q -branch transitions) are also allowed as are transitions with $\Delta K_a = \pm 2$. But these transitions are much weaker than the strong R -branch transitions because of the proximity of κ to -1 and none have been identified for excited vibrational states.

Isotopologues with two H (and also those with two D) have C_{2v} symmetry. Three of the six fundamental vibrations are in the totally symmetric symmetry class A_1 , one is in B_1 and two are in B_2 with transition dipole moments μ_a , μ_c and μ_b respectively. The two equivalent H nuclei in H₂CS and H₂C³⁴S lead to *ortho* and *para* spin-statistics with a 3 : 1 weight ratio. The *ortho* states are described by K_a being odd in vibrational states of A symmetry whereas K_a is even in B symmetry states.

The origins of the CH₂ stretching states $v_1 = 1$ and $v_5 = 1$ are at 2971.03 and 3024.62 cm⁻¹, respectively, for the H₂CS main isotopologue [21]. Rotational transitions within these states are weaker than a factor of 10⁻⁶ at 300 K compared with the ground vibrational states and hence unobservable in normal absorption spectra. Rotational transitions of the remaining fundamental vibrational states have been identified in the course of our investigations. The state $v_2 = 1$ at 1455.496 cm⁻¹ is the CH₂ bending state while $v_3 = 1$ at 1059.205 cm⁻¹ is the CS stretching state. Their Boltzmann factors at 300 K are 9.3×10^{-4} and 6.2×10^{-3} , respectively, while those of the out-of-plane state $v_4 = 1$ at 990.183 cm⁻¹ and of the CH₂ rocking state $v_6 = 1$ at 991.020 cm⁻¹ are about 8.6×10^{-3} . The near-degeneracy of two states with one more state close by and another one somewhat more distant make the low-lying fundamentals of thioformaldehyde a textbook example of Coriolis coupling. The interactions of $v_4 = 1$ with $v_2 = 1$ or $v_3 = 1$ obey b -type selection rules, meaning that $\Delta J = 0$, ΔK_a and ΔK_c are odd. The interactions of $v_6 = 1$ with $v_2 = 1$ or $v_3 = 1$ follow c -type selection rules with $\Delta J = 0$, ΔK_a odd and ΔK_c even. No interactions occur between $v_2 = 1$ and $v_3 = 1$ because they are in the same symmetry class

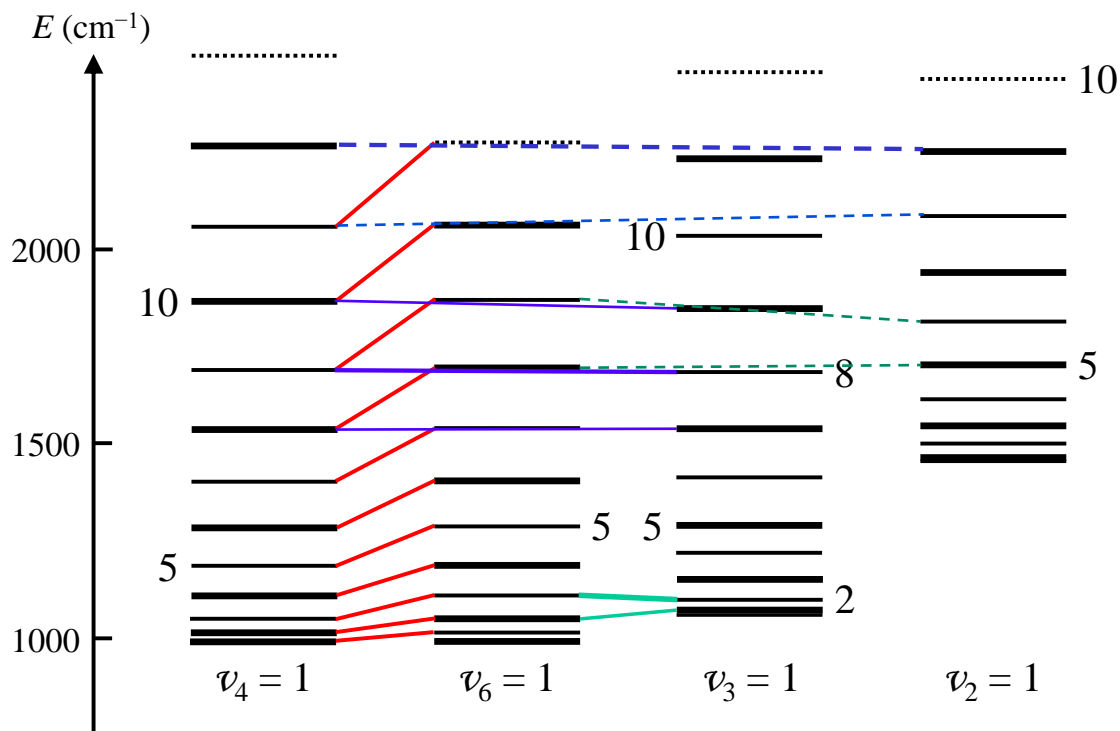


Figure 1. Diagram showing the K_a energy level of the four lowest excited vibrational states of H_2CS . Black solid lines indicate levels accessed in the present investigation, dotted ones the first level not accessed; *ortho* levels are indicated by thicker lines. Please note that the lines for $K_a = 0$ and 1 are often not separated. Red, blue and green lines signal (near-) resonant *a*-, *b*- and *c*-type Coriolis interactions, respectively. Solid lines stand for $\Delta K_a = 0$ or 1 interactions, dashed lines for $\Delta K_a = 3$ interactions.

while *a*-type selection rules govern the interactions between $\nu_4 = 1$ and $\nu_6 = 1$.

Figure 1 displays the K_a level structure of $\nu_4 = 1$, $\nu_6 = 1$, $\nu_3 = 1$ and $\nu_2 = 1$ from left to right with *ortho*-levels marked by thicker lines; (near-) resonant Coriolis interactions are indicated with coloured lines. Coriolis interactions in a strict sense are interactions between fundamental vibrational states as well as interactions between vibrational states where a particular number of vibrational quanta have been added to both of these interacting vibrational states. Equivalent interactions in a more general sense are called rotational resonances because the strength of the interaction scales with J and K .

The most striking feature in the K_a energy level diagram is the *a*-type interaction between the two essentially degenerate states $\nu_4 = 1$ and $\nu_6 = 1$. The K_a levels repel each other with increasing K_a starting from $K_a = 1$ as the selection rules involve $\Delta K_a = 0$. The asymmetry splitting causes the interaction between the upper asymmetry level of a particular K_a of $\nu_4 = 1$ with the lower asymmetry level of the same K_a of $\nu_6 = 1$ to be stronger than the interaction between the lower asymmetry level of $\nu_4 = 1$ with the upper asymmetry level of $\nu_6 = 1$ because the latter pair of levels is farther apart than the former. The asymmetry splitting in $\nu_4 = 1$ is inverted in frequency and in energy at lower values of J as a consequence and both $K_a = 1$ levels of $\nu_4 = 1$ are lower in energy than $K_a = 0$ up to $J = 6$. The assignments to the upper asymmetry level of $\nu_4 = 1$ and the lower asymmetry level of $\nu_6 = 1$ swap at some higher value of J . The asymmetry splitting in an unperturbed vibrational state is largest in $K_a = 1$ so this swap in assignment occurs in the H_2CS isotopologue already at $J = 7$, at $J = 23$ for $K_a = 2$ and at $J = 44$ for $K_a = 3$.

The $\nu_3 = 1$ state is perturbed through *c*-type Coriolis interaction with $\nu_6 = 1$ at low values of K_a with $K_a = 2$ of $\nu_3 = 1$ being very close to $K_a = 3$ of $\nu_6 = 1$ in particular at low values of J , see Fig. 1; $K_a = 1$ of $\nu_3 = 1$ get very close to $K_a = 2$ of $\nu_6 = 1$ at higher values of J with a resonant $\Delta K_c = 2$ crossing in energy between $J = 39$ and 40. More resonant crossings occur

beyond the range of J values covered in the present study. Perturbations of higher values in K_a of $v_3 = 1$ occur through $\Delta K_a = 1$ b -type Coriolis interaction with $v_4 = 1$ and $K_a = 7$ to 9 of $v_3 = 1$ interacting most strongly with $K_a = 8$ to 10 of $v_4 = 1$. A resonant crossing in energy occurs for $K_a = 8$ of $v_3 = 1$ and $K_a = 9$ of $v_4 = 1$ between $J = 30$ and 31.

The vibrational energy of $v_2 = 1$ is substantially higher than those of the lowest three excited vibrational states. Interactions with $v_4 = 1$ and $v_6 = 1$ involve near-degeneracies of b - and c -type selection rules with $\Delta K_a = 3$ as is demonstrated in Fig. 1. Levels with $K_a = 9$ of $v_2 = 1$ and $K_a = 12$ of $v_4 = 1$ are somewhat close in energy while $K_a = 8$ of $v_2 = 1$ and $K_a = 11$ of $v_4 = 1$ are less close in energy. Levels with $K_a = 5$ of $v_2 = 1$ and $K_a = 8$ of $v_6 = 1$ as well as those with $K_a = 6$ of $v_2 = 1$ and $K_a = 9$ of $v_6 = 1$ are also comparatively close in energy.

4. Analysis and fitting

Assignments in the OSU FASSST spectra of thioformaldehyde were carried out with the Computer Aided Assignment of Asymmetric Rotor Spectra (CAAARS) program applying the Loomis–Wood procedure, with which an observed spectrum is visually compared with calculated line positions and intensities to make new assignments [57]. The software facilitates user-defined sorting of predicted transitions into branches. It then overlays consecutive transitions into a Loomis–Wood diagram, thus, aiding visual search for matching lines between predictions and experiment.

Calculation and fitting of spectra were carried out with Pickett’s SPCAT and SPFIT programs [58]. It is important to apply the assignment option ”eigenvector sort of states” instead of the default ”energy sort of Wang sub-blocks” in cases with pronounced first-order Coriolis coupling. An informative example is the $v_8 = 3$ $l = +3$ substate in which K levels decrease from $K = 0$ because of the strong Coriolis interaction with the $l = -3$ substate to $K = 3$ and only $K \geq 6$ are higher in energy than $K = 0$ [59]. The option ”eigenvector sort of states” secures this labelling. Additional aspects of the labelling of K quantum numbers in SPCAT and SPFIT are available elsewhere [58].

Watson’s S reduction was employed in the rotational Hamiltonian. It is more versatile in general and obviously more appropriate than the A reduction in the case of thioformaldehyde because of the proximity to the symmetric prolate limit. The centrifugal distortion parameters in an excited vibrational state of a fairly rigid molecule are often quite close to those in the ground vibrational state. We apply the ground state rotational parameters X_0 of H_2CS or of $\text{H}_2\text{C}^{34}\text{S}$ to all excited vibrational states and introduce differences $\Delta X_i = X_i - X_0$ as far as needed; i represents an excited vibrational state. This approach has several advantages of which the most important ones are first the ground state centrifugal distortion parameters account commonly to a considerable amount for the distortion effects in an excited vibrational state and second it is easier to recognise if a particular ΔX_i is determined with sufficient significance. Both aspects may help to reduce the number of spectroscopic parameters to reach a satisfactory fit. And finally large parameters ΔX_i and ΔX_j of two vibrational states of similar magnitudes and opposite signs may indicate an unaccounted perturbation.

To keep the parameter set small and somewhat unique we test after each round of assignments if the use of a particular parameter improves the rms error of the fit as a measure of the quality of the fit. We search among the meaningful parameters for the one that improves the rms error most. The parameter is kept in the fit if the improvement is deemed to be sufficient and if the parameter is determined with significance. The procedure is repeated until improvements of the fit are marginal at most. This fitting strategy works usually very well for molecules close to the prolate symmetric limit, but occasionally less well for very asymmetric rotors or rotors closer to the oblate symmetric limit.

The vibration–rotation interaction between two vibrational states is commonly treated with a Hamiltonian that can be divided into a 2×2 matrix with the diagonal elements consisting usually of two Watson-type rotational Hamiltonians, including the vibrational energy of each state, and the interaction Hamiltonian off-diagonal. This procedure is extended analogously in

cases of several interacting vibrational states.

The low order Coriolis terms of a -symmetry are

$$iG_a J_a + F_{bc} \{J_b, J_c\}$$

with $\{, \}$ being the anticommutator; terms of b - and c -symmetry are defined equivalently. We point out that other designations than G and F may be found, in particular in the older literature. One of the early and well-recognised examples to establish that both terms are not only allowed but also needed was a study of the c -symmetry Coriolis interaction between $v_1 = 1$ and $v_3 = 1$ in ozone [60]. These terms may be supplemented with distortion corrections of the type

$$i(G_{a,K} J_a^3 + G_{a,J} \{J_a, J^2\} + G_{2a} \{J_a, J_b^2 - J_c^2\} + \dots)$$

and

$$F_{bc,K} \{J_a^2, \{J_b, J_c\}\} + F_{bc,J} J^2 \{J_b, J_c\} + F_{2bc} (J_b^2 - J_c^2) \{J_b, J_c\} + \dots$$

in the case of a prolate representation. Such terms were required extensively for example in the treatment of the Coriolis interaction of $v_4 = 1$ and $v_6 = 1$ in ClClO_2 [61]. The sign of G_a coupling two specific vibrations is usually not determinable through a fit. Its sign may, however, affect the intensities of some rotational or rovibrational transitions in conjunction with the signs of permanent or transition dipole moment components. The signs of F_{bc} or of distortion corrections to G_a or F_{bc} are determinable in fits relative to the sign of G_a .

In the case of Coriolis interaction between two fundamental vibrations ν_x and ν_y the associated $G_i(x, y)$ can be evaluated through

$$G_i(x, y) = \zeta_{x,y}^i B_e^i \left(\sqrt{\frac{\omega_x}{\omega_y}} + \sqrt{\frac{\omega_y}{\omega_x}} \right)$$

where ω_x and ω_y are the corresponding harmonic vibrations, B_e^i is the i -axis equilibrium rotational parameter and $\zeta_{x,y}^i$ a Coriolis term that can be evaluated from a harmonic force field calculation. Replacing ω_x and ω_y with ν_x and ν_y has usually only a small effect whereas the substitution of B_e^i by B_0^i may lead to a more pronounced change. Vibration–rotation interaction frequently increases correlation in the fitting procedure. Fixing one or more G_i to values from a force field calculation is a way to reduce correlation in cases of Coriolis interaction and results usually in physically more meaningful values for the remaining parameters compared to cases in which the G_i are floated or kept fixed at zero. Fixing to values derived from a force field calculation is also advisable if the experimental data set does not reach the quantum number range of strongest interactions, usually for levels of the interacting vibrations with $\Delta K_a = 0$ for a -type interaction and $\Delta K_a = 1$ for b - or c -type interaction in case of a prolate rotor. This was done for example for G_a and G_b in the case of $v_4 = 1$ and $v_6 = 1$ in ClClO_2 [61] or for G_c in the case of $v_1 = 1$ and $v_3 = 1$ in SO_2 [62].

We carried out quantum-chemical calculations at the Regionales Rechenzentrum der Universität zu Köln (RRZK) to evaluate $\zeta_{x,y}^i$ and ν_x for H_2CS and $\text{H}_2\text{C}^{34}\text{S}$. We applied MP2 Møller–Plesset perturbation theory of second order [63] using a correlation-consistent basis set of quadruple zeta quality augmented with diffuse and tight core-correlating basis functions designated as aug-cc-pwCVQZ [64, 65]. We resorted to the commercially available program Gaussian 16 [66] and applied the default frozen core option.

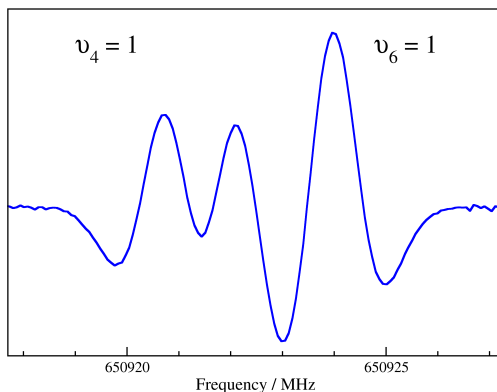


Figure 2. Spectral recording of H_2CS displaying the $J = 19 - 18$ transitions with $K_a = 4$ of $\nu_4 = 1$ and $\nu_6 = 1$. The $\nu_4 = 1$ splitting is inverted whereas the $\nu_6 = 1$ splitting is not resolved.

5. Results

We describe in the following our results obtained for the four lowest excited vibrational states of H_2CS and $\text{H}_2\text{C}^{34}\text{S}$ and the contribution to the ground vibrational state of $\text{H}_2\text{C}_2\text{S}$.

5.1. H_2CS

The Loomis–Wood display of the OSU spectral recordings revealed several unassigned series in K_a that were slightly weaker than those of H_2^{13}CS and that resembled more or less those of H_2CS after having assigned transitions of several thioformaldehyde isotopologues [32]. It was quite natural to assume these are caused by low-lying excited vibrational states of H_2CS . This assumption was easily verified applying spectroscopic parameters from two older IR studies in which combined analyses of ν_4 , ν_6 and ν_3 were presented and the Coriolis interaction was analysed as far as it is present in their data [23, 24]. Transitions within $\nu_2 = 1$ could be assigned subsequently based on an IR investigation of ν_2 that treated the band as unperturbed despite indications to the contrary [22].

The OSU measurements cover $J = 4 - 3$ to $10 - 9$ or $11 - 10$ encompassing the $J = 7 - 6$ transitions between $\nu_4 = 1$ and $\nu_6 = 1$ having $K_a = 1$ and $K_c = J - K_a$ in the case of $\nu_4 = 1$ (the upper asymmetry component in an unperturbed vibrational state) and $K_c = J - K_a + 1$ in the case of $\nu_6 = 1$ (the lower asymmetry component). The associated transitions within $\nu_4 = 1$ or $\nu_6 = 1$ were not calculated at a threshold more than a factor of 1000 lower. The assignments extended to $K_a = 8$ for $\nu_4 = 1$ and $\nu_6 = 1$, to $K_a = 7$ for $\nu_3 = 1$ and to $K_a = 6$ for $\nu_2 = 1$. Uncertainties of 50 kHz were attributed to all of the excited state lines of H_2CS from OSU.

It may be useful to describe qualitatively how the rotational of H_2CS in low-lying excited vibrational states appear in comparison to the ground vibrational state. We describe the general features of the $J = 10 - 9$ transition as it was contained in the OSU recordings. The $K_a = 3$ to 9 lines of $\nu = 0$ cover sequentially from ~ 343.4 GHz down to 342.6 GHz with the $K_a = 2$ lines to either side of the $K_a = 3$ lines and the $K_a = 1$ lines near 338.1 and 348.5 GHz. The appearance of $\nu_2 = 1$ is quite similar. The transitions of $\nu_4 = 1$ and $\nu_6 = 1$ occur in much smaller frequency regions. The $K_a = 2$ to 8 lines of $\nu_4 = 1$ occur sequentially from about 343.3 to 341.5 GHz with $K_a = 0$ and 1 near $K_a = 6$ and $K_a = 9$ more than 3 GHz lower than $K_a = 8$. The $K_a = 3$ to 9 lines of $\nu_6 = 1$ cover sequentially essentially the same region as most of the $\nu_4 = 1$ lines, one of the $K_a = 1$ lines slightly higher and the remaining low- K_a lines distributed among the higher K_a ones. Finally, the $\nu_3 = 1$ lines occur in a very irregular way. The $K_a = 1$ lines are found at the upper and lower end, as one would expect, separated by almost exactly 10 GHz; $K_a = 9$ appears roughly 2 GHz above the lower of the $K_a = 1$ lines and $K_a = 8$ roughly 2 GHz below the upper $K_a = 1$ line.

After having fitted the OSU excited vibrational state data of H₂CS well it was straightforward to locate transitions at higher frequencies in Cologne. The BWO measurements between 566 and 670 GHz and between 848 and 930 GHz cover $J = 17 - 16$ to $19 - 18$ and $J = 25 - 24$ to $27 - 26$ for as many K_a values of the four excited vibrational states as possible. The extent of the coverage differs for various reasons. One very obvious reason is that the intensity drops with increasing K_a , though moderated by the spin statistics, and with vibrational energy. Further reasons are blending with other lines, the proximity of much stronger lines, the drop in sensitivity of the BWO or difficulty to lock the BWO. The K_a quantum numbers reach 12 (11) for $v_4 = 1$, 10 (8) for $v_6 = 1$, 11 for $v_3 = 1$ and 9 (7) for $v_2 = 1$ where the numbers in parentheses refer to the 848–930 GHz region, see also Fig. 1. The different asymmetry splitting in $K_a = 4$ of $v_4 = 1$ and $v_6 = 1$ is shown in Fig. 2 for $J = 19 - 18$. The $v_4 = 1$ asymmetry splitting is inverted meaning that the transition with $K_c = J + K_a$ is below the one with $K_c = J + K_a + 1$ whereas it is opposite in unperturbed vibrational states. The asymmetry splitting in $v_4 = 1$ is -1.29 MHz (the minus sign indicates the inverted splitting) whereas the unresolved splitting in $v_6 = 1$ is calculated to be 0.09 MHz. The observed or calculated values in $v = 0$, $v_3 = 1$ and $v_2 = 1$ are 1.31, 1.13 and 1.79 MHz, respectively, for comparison purpose.

Measurements in the 1290–1390 GHz region were carried out some time later. They cover $J = 37 - 36$ to $41 - 40$. No attempts were made to record transitions of $v_2 = 1$ in the upper frequency region because the Boltzmann peak of the rotational spectrum of thioformaldehyde is near 820 GHz at 300 K and because of the lower power of the source compared to the BWOs. Nevertheless, $K_a = 8$ was reached for $v_4 = 1$ with no coverage of the *para* levels with $K_a = 5$ and 7. Levels with $K_a \leq 3$ and $K_a = 6$ were covered in $v_6 = 1$ and levels with $K_a \leq 3$ and $K_a = 7$ were covered in $v_3 = 1$. We obtained in particular transition frequencies for $J = 40 - 39$ transitions between $v_6 = 1$ and $v_3 = 1$ having $K_a = 2$ and $K_c = J - K_a$ in $v_6 = 1$ and $K_a = 1$ and $K_c = J - K_a + 1$ in $v_3 = 1$. The associated transitions within $v_6 = 1$ or $v_3 = 1$ were calculated to be around a factor of 50 weaker, too weak to be observed in a reasonable time and possibly difficult to identify because of the huge amount of lines of similar or larger intensities. Other resonant crossings in energy mentioned in Section 3 were in measurement gaps of the Cologne measurements or beyond the upper frequency limit. Uncertainties of 5 to 10 kHz were assigned to very symmetric lines with good or very good S/N, less symmetric lines or lines with somewhat lower S/N were deemed to be more uncertain up to 70 kHz.

The excited state data of H₂CS from OSU and from the Universität zu Köln were fitted together with the previously published ground state data [32], as well as transition frequencies for ν_4 and ν_6 [23, 24], ν_3 [23] and ν_2 [22] in our first combined fit. Uncertainties of 0.001 cm^{-1} were assigned to the laser Stark data [23], 0.01 cm^{-1} to the ν_4 and ν_6 data [24] and 0.0005 cm^{-1} initially to the ν_2 data [22] roughly based on the average residuals in the initial fits. The uncertainties of the ν_2 data were reduced in the final fits to 0.00035 cm^{-1} . We obtained the ν_2 data from the corresponding author as they were not available anymore as supplementary material through the journal.

We encountered labelling issues in particular in the laser Stark study [23]. The ν_3 transitions should obey *a*-type selection rules with $\Delta K_a = 0$ and $\Delta K_c = \pm 1$. They were mentioned as *a*-type transitions in the text but were frequently given as *x*-type transitions with $\Delta K_a = \Delta K_c = 0$ in the table. The applied Stark field and also the Lamb-dip technique, which was used for several transitions, may introduce intensities to otherwise forbidden transitions. We have attributed the assignments to allowed transitions wherever this appeared to be appropriate but retained assignments where this would cause too large residuals in the fit or if an allowed and a forbidden transition with similar quantum numbers were reported. It was necessary in other cases to modify K_c or K_a or both, also in the FTIR study of ν_4 and ν_6 [24], or to modify the vibrational assignments. Two $K_a = 1 - 0$ *Q*-branch transitions of ν_4 [23] were reassigned from $J = 1$ and 2 to $J = 2$ and 4. Several own lines were omitted in the ν_2 FTIR study. We included all but two in our fit and point out that some of the lines fitted better because they were treated as unresolved asymmetry doublets in our fit whereas only one line each was given in the initial line list. We omitted six and three transition frequencies from the laser Stark study [23] and from the ν_4 and ν_6 investigation [24], respectively, because of large residuals.

Table 1. Ground state spectroscopic parameters (MHz) of H₂CS from previous rotational study (rot)^a and from combined fits with old (combined1)^b and new (combined2)^c data of ν_4 , ν_6 and ν_3 along with H₂C³⁴S parameters.

Parameter	H ₂ CS			H ₂ C ³⁴ S
	rot	combined1	combined2	
$A - (B + C)/2$	274437.5932 (115)	274437.5891 (113)	274437.6073 (110)	274729.46 (19)
$(B + C)/2$	17175.745955 (196)	17175.746282 (147)	17175.746270 (146)	16882.911660 (111)
$(B - C)/4$	261.6240523 (165)	261.6240459 (165)	261.6240453 (165)	252.793065 (73)
$D_K \times 10^3$	23343.78 (164)	23342.99 (160)	23346.11 (154)	23625. (58)
$D_{JK} \times 10^3$	522.2938 (43)	522.3013 (40)	522.2957 (40)	504.8472 (48)
$D_J \times 10^6$	19018.75 (39)	19019.24 (27)	19019.28 (27)	18404.267 (136)
$d_1 \times 10^6$	-1208.429 (105)	-1208.557 (92)	-1208.534 (92)	-1148.572 (108)
$d_2 \times 10^6$	-177.3270 (222)	-177.3113 (215)	-177.3077 (214)	-165.659 (120)
$H_K \times 10^3$	5.946 (35)	5.914 (34)	5.954 (33)	6.00
$H_{KJ} \times 10^6$	-28.155 (86)	-28.071 (83)	-28.194 (82)	-28.027 (106)
$H_{JK} \times 10^6$	1.50409 (270)	1.50752 (236)	1.50744 (235)	1.41855 (70)
$H_J \times 10^9$	-5.81 (32)	-5.51 (21)	-5.50 (21)	-4.913 (40)
$h_1 \times 10^9$	3.018 (141)	3.222 (120)	3.190 (120)	2.765 (36)
$h_2 \times 10^9$	1.6472 (140)	1.6374 (135)	1.6373 (135)	1.412 (49)
$h_3 \times 10^9$	0.3619 (73)	0.3739 (68)	0.3763 (68)	0.3151 (99)
$L_K \times 10^6$	-2.109 (206)	-1.903 (200)	-2.056 (194)	-2.09
$L_{KKJ} \times 10^9$	-21.36 (69)	-21.69 (67)	-20.84 (67)	-20.92 (63)
$L_{JK} \times 10^9$	0.2032 (90)	0.1855 (82)	0.1883 (82)	0.183
$L_{JJK} \times 10^{12}$	-10.32 (81)	-10.66 (71)	-10.73 (71)	-9.4
$L_J \times 10^{12}$	0.833 (87)	0.767 (58)	0.766 (58)	0.65
$l_1 \times 10^{12}$	-0.358 (47)	-0.432 (40)	-0.421 (40)	-0.35
$P_{KKJ} \times 10^{12}$	-18.63 (180)	-18.11 (177)	-20.03 (175)	-19.8

Notes: Watson's S reduction was used in the representation I' . Numbers in parentheses are one standard deviation in units of the least significant figures. Parameters without uncertainties were estimated and kept fixed in the analyses. See also Section 5.1 for further details.

^aRef. [32]

^bGround state data from Ref. [32] and IR data from Refs. [22–24].

^cGround state data from Ref. [32] and IR data from Refs. [22, 25].

The parameter set was assembled starting from first-order Coriolis parameters from a quantum-chemical calculation. The values applied in intermediate fits were close to available values, but did not agree with any particular set. Therefore, the final values were taken from an MP2/aug-cc-pwCVQZ calculation as indicated in Section 4. Initial parameters ΔX were evaluated from previous work [22–24] as were estimates of the vibrational energies. The need for fitting any of the first-order Coriolis parameters was evaluated frequently. It became clear rather quickly that it was necessary to fit $G_a(4,6)$ and $G_c(3,6)$. The situation was more complex in the case of $G_b(3,4)$. Trial fits in a late stage of the fitting process yielded values close to the initial one with reasonable uncertainties of ~ 9 MHz, however, uncertainties not only of $\Delta(B + C)/2$ and $\Delta(B - C)/4$ of $\nu_3 = 1$ and $\nu_4 = 1$ increased substantially but through correlation also those of $\Delta(A - (B + C)/2)$ of $\nu_4 = 1$ and $\nu_6 = 1$ among several others and their values changed well outside the larger uncertainties. Therefore, $G_b(3,4)$ was kept fixed to the initial value in the latest fits.

It turned out in the fitting process that the signs of the $G_i(x, y)$ cannot be changed independently of each other without significant deterioration of the quality of the fit. A sign change in $G_b(2,4)$ afforded a sign change in $G_c(2,6)$ if the sign of $G_a(4,6)$ was retained; the same applied to $G_b(3,4)$ and $G_c(3,6)$. If, however, the sign of $G_a(4,6)$ was changed it was necessary to change the signs of two other combinations of $G_b(x, y)$ or $G_c(x, y)$.

There appeared to be no dependence of the intensities of the rotational transitions upon sign change of the $G_i(x, y)$ among transitions having similar intensities as the observed ones. But in part substantial intensity modifications were calculated in the IR spectrum upon sign change of the $G_i(x, y)$. Applying the quantum-chemically calculated transition dipole moments as positive for four fundamental vibrations from Ref. [38] slightly adjusted to take into account the experimental transition dipole moment ratios for the lower three fundamentals [25] it was fairly obvious from relative intensities in several ν_4 and ν_6 Q -branch transitions that $G_a(4,6)$ has to be negative. The P -branch of ν_2 appears to be slightly stronger than the R -branch according to Fig. 1 of Ref. [22], affording $G_b(2,4)$ and in turn $G_c(2,6)$ to be positive. The effects

Table 2. Vibrational energies E (cm^{-1}) and changes ΔX of spectroscopic parameters (MHz) of H_2CS in excited vibrational states employing the old data of ν_4 , ν_6 and ν_3 .

Parameter	$\nu_4 = 1$	$\nu_6 = 1$	$\nu_3 = 1$	$\nu_2 = 1$
E	990.182542 (128)	991.020175 (127)	1059.204930 (123)	1455.495737 (25)
$\Delta(A - (B + C)/2)$	-143.59 (49)	632.82 (40)	-222.176 (281)	2510.097 (113)
$\Delta(B + C)/2$	-3.198890 (229)	-11.07153 (50)	-108.05638 (58)	-26.976754 (233)
$\Delta(B - C)/4$	-5.03832 (158)	12.52173 (167)	-0.990805 (274)	6.931217 (282)
$\Delta D_K \times 10^3$	666.3 (264)			2041.9 (26)
$\Delta D_{JK} \times 10^3$	-4.983 (284)	2.655 (126)	-2.641 (72)	23.771 (287)
$\Delta D_J \times 10^6$	190.75 (59)	105.20 (46)	158.69 (44)	-105.09 (59)
$\Delta d_1 \times 10^6$	-11.249 (296)	-85.92 (37)	-19.914 (184)	
$\Delta d_2 \times 10^6$		-33.259 (210)	-6.568 (72)	
$\Delta H_{KJ} \times 10^6$	7.75 (39) ^a	7.75 (39) ^a		-12.64 (91)
$\Delta H_J \times 10^9$		-0.436 (125)	1.811 (105)	
$\Delta h_1 \times 10^9$		1.594 (113)		

Notes: Watson’s S reduction was used in the representation I^r . $\Delta X = X_{\text{vib}} - X_0$. Numbers in parentheses are one standard deviation in units of the least significant figures. Empty fields indicate ΔX was not used in the final analysis.

^aConstrained to be equal, see Section 5.1.

of sign changes of $G_b(3,4)$ and $G_c(3,6)$ on the intensities are relatively similar but occur in a more crowded region of the spectrum. The choice of $G_b(3,4)$ being negative and $G_c(3,6)$ being positive appears to be in better agreement with the experimental spectrum [25] than the opposite sign choice.

Several ΔX were determined besides the vibrational energies for all four excited vibrational states. The selection differed among the states; most or all quartic ΔX were employed together with up to three of the seven sextic ΔX . The parameters $\Delta(A - (B + C)/2)$ and ΔD_{JK} of $\nu_4 = 1$ and $\nu_6 = 1$ are of similar magnitude, but opposite sign. Even though they are comparatively small with respect to the corresponding ground state parameter omission of one caused a considerable deterioration of the quality of the fit that could not be easily accounted for otherwise. The ΔH_{KJ} for these states were comparatively large and only moderately well determined. Their values did not change significantly if only one of the two or both were employed in the fit. The values were constrained to be the same as a consequence. It was not possible to determine ΔD_K significantly for $\nu_6 = 1$ and for $\nu_3 = 1$. Several sextic distortion parameters were tested but many resulted in improvements that were largely negligible. The effect of $\Delta H_{J,6}$ was larger in some intermediate fits and more on the edge in the final fit. Diverse sets of distortion corrections to the $G_i(x, y)$ were used in the fits, fairly large sets for $G_a(4,6)$ and $G_c(3,6)$ and no correction to $G_c(2,6)$. There was no evidence for the need of any of the $F_{j,k}(x, y)$ in the fits.

The ground state rotational parameters from the final fit are given in Table 1 together with those from our previous ground state study [32], values from a second combined fit and values from a combined fit of $\text{H}_2\text{C}^{34}\text{S}$ data. The ΔX_i from this fit are presented in Table 2 while those of the second combined fit are gathered in Table 3. The interaction parameters from both fits as well as those from the $\text{H}_2\text{C}^{34}\text{S}$ fit are finally given in Table 4.

We became aware of an extensive high-resolution investigation of H_2CS in the $10\mu\text{m}$ region covering the ν_4 , ν_6 and ν_3 bands [25] at a relatively early stage of our own research and received a line list from one of the authors prior to publication. The interactions between the three excited vibrational states were taken into account as in earlier publications [23, 24] but the effects of perturbations originating from $\nu_2 = 1$ were not considered even though a high-resolution study had been published in the meantime [22]. We replaced the older ν_4 , ν_6 and ν_3 data with the new ones in order to evaluate the impact of these new data. We encountered massive labelling problems in that data set which have been discussed in a recent evaluation of experimental H_2CS data [33]. Most mislabellings were encountered among the ν_4 and ν_6 at moderate and higher K_a ($\gtrsim 2$). The vibrational identifier and the K_c value had to be modified. It was necessary for some higher values of J to decrease K_a by 2 and raise K_c by 2 compared with modifications at lower J . This was particularly peculiar in cases of unresolved asymmetry doublets in which one transition had the correct value of K_a and one had a higher one by 2. There appear to be no labelling issues in the ν_3 data. One of the transitions was reassigned and eight transition

Table 3. Vibrational energies E (cm^{-1}) and changes ΔX of spectroscopic parameters (MHz) of H_2CS in excited vibrational states employing the new data of ν_4 , ν_6 and ν_3 .

Parameter	$\nu_4 = 1$	$\nu_6 = 1$	$\nu_3 = 1$	$\nu_2 = 1$
E	990.182588 (19)	991.020207 (19)	1059.205183 (17)	1455.495737 (25)
$\Delta(A - (B + C)/2)$	-142.529 (245)	634.741 (242)	-222.955 (106)	2510.094 (113)
$\Delta(B + C)/2$	-3.198386 (213)	-11.07162 (49)	-108.05631 (57)	-26.977124 (226)
$\Delta(B - C)/4$	-5.04129 (147)	12.51873 (156)	-0.990983 (268)	6.931084 (280)
$\Delta D_K \times 10^3$	771.77 (213)		-26.81 (230)	2041.0 (26)
$\Delta D_{JK} \times 10^3$	-5.505 (265)	2.565 (123)	-2.604 (70)	24.477 (260)
$\Delta D_J \times 10^6$	190.50 (58)	105.92 (46)	157.76 (44)	-105.08 (59)
$\Delta d_1 \times 10^6$	-11.394 (295)	-85.58 (36)	-20.321 (162)	
$\Delta d_2 \times 10^6$		-33.150 (196)	-6.471 (69)	
$\Delta H_{KJ} \times 10^6$	8.58 (38) ^a	8.58 (38) ^a		-14.07 (89)
$\Delta H_J \times 10^9$		-0.452 (122)	1.748 (103)	
$\Delta h_1 \times 10^9$		1.540 (112)		

Notes: Watson's S reduction was used in the representation I^r . $\Delta X = X_{\text{vib}} - X_0$. Numbers in parentheses are one standard deviation in units of the least significant figures. Empty fields indicate ΔX was not used in the final analysis.

^aConstrained to be equal, see Section 5.1.

frequencies were omitted because of large residuals between reported frequencies and those calculated from the final fit. One line is a $K_a = 8$ Q -branch line in ν_3 , however, Table 1 of Ref. [25] states $K_a \leq 7$ in ν_3 . Five omitted transition frequencies are $K_a = 10 - 9$ R -branch transition in ν_6 correctly indicated in Table 1 of Ref. [25] but not in the line list.

We assigned uncertainties of 0.0007 cm^{-1} to the majority of the lines initially as suggested by the reported rms of the fit of exactly this value [25]. Some uncertainties were larger by a factor of 2 or 4 in accordance with indications in the line list. The uncertainties were reduced to 0.0005 cm^{-1} and factors of 2 or 4 larger in the final fits. This data set required two additional parameters $\Delta D_{K,3}$ and $G_{a,KKK}(4,6)$ besides the ones already employed to fit the old ν_4 , ν_6 and ν_3 data. We also tried to include these old IR data in the fit. While the data sets were compatible with each other the parameter values and their uncertainties changed insignificantly such that we omitted the old ν_4 , ν_6 and ν_3 data in the final second combined fit.

As indicated before, the ground state rotational parameters from this second combined fit are also in Table 1. The ΔX_i from this fit are given in Table 3 and the interaction parameters are given in Table 4.

The new set of ν_4 , ν_6 and ν_3 data [25] consists of 3442 transitions corresponding to 2482 different lines with J/K_a extending to 41/8, 35/8 and 34/7, respectively, and was fitted to 0.00048 cm^{-1} . The 599 ν_2 transitions [22] conform to 436 different lines with $J \leq 37$ and $K_a \leq 7$ and were reproduced in both fits to 0.00035 cm^{-1} , also within the uncertainties on average. The 80 ν_4 , ν_6 and ν_3 transitions (70 lines) from a laser Stark study [23] with J/K_a reaching 13/3, 12/2 and 6/5, respectively, had an rms of 0.00105 cm^{-1} and the 376 transitions (224 lines) from an older FTIR investigation of ν_4 and ν_6 [24] extend to J/K_a of 25/5 and 24/8, respectively, were reproduced to 0.0106 cm^{-1} ; this is in both cases marginally above the attributed uncertainties. The 372 OSU rotational transitions (280 lines) cover $3 \leq J \leq 11$ and $K_a \leq 8$, 8, 7 and 6 for $\nu_4 = 1$, $\nu_6 = 1$, $\nu_3 = 1$ and $\nu_2 = 1$, respectively, with rms values of 50.7 kHz in the first combined fit and 51.4 kHz in the second combined fit, marginally above the assigned uncertainties. The measurements at the Universität zu Köln resulted in 406 transition corresponding to 301 different lines with $16 \leq J \leq 41$ for $\nu_4 = 1$, $\nu_6 = 1$ and $\nu_3 = 1$ while $16 \leq J \leq 27$ in the case of $\nu_2 = 1$. The K_a quantum numbers reached 12, 10, 11 and 9 for $\nu_4 = 1$, $\nu_6 = 1$, $\nu_3 = 1$ and $\nu_2 = 1$, respectively. The rms of 26.3 kHz in the first combined fit and 24.2 kHz in the second combined fit were on average slightly and marginally above the assigned uncertainties, respectively.

Table 4. Interaction parameters (MHz) of H₂CS from from combined fits with old (combined1)^a and new (combined2)^b data of ν_4 , ν_6 and ν_3 along with H₂C³⁴S interaction parameters.

Parameter	H ₂ CS		H ₂ C ³⁴ S
	combined1	combined2	
	$v_4 = 1/v_6 = 1$		
G_a	-300209.33 (40)	-300211.424 (130)	-299919.0 (90)
$G_{a,K}$	58.371 (42)	58.7267 (147)	58.76
$G_{a,J} \times 10^3$	867.1862 (271)	867.1433 (264)	842.702 (200)
$G_{a,KK} \times 10^3$	-29.24 (88)	-31.24 (38)	-31.3
$G_{a,JK} \times 10^6$	616.8 (40)	615.2 (39)	605.
$G_{a,KKK} \times 10^6$		37.47 (288)	37.6
$G_{a,JKK} \times 10^9$	674.3 (180)	658.5 (175)	648.
$G_{a,JJK} \times 10^9$	-4.82 (35)	-5.32 (35)	-5.2
$G_{2a} \times 10^3$	-416.07 (234)	-422.20 (219)	-408.
$G_{4a} \times 10^6$	-7.214 (177)	-7.211 (171)	-6.7
	$v_2 = 1/v_4 = 1$		
G_b	30660.	30660.	30118.
$G_{b,K}$	10.196 (125)	10.498 (113)	10.33
$G_{b,J} \times 10^3$	-65.379 (262)	-65.193 (259)	-62.9
$G_{2b} \times 10^3$	42.271 (125)	42.455 (120)	40.3
	$v_3 = 1/v_4 = 1$		
G_b	-2177.	-2177.	-2172.
$G_{b,J} \times 10^3$	-97.857 (56)	-97.818 (56)	-95.92
$G_{b,JJ} \times 10^6$	1.2886 (131)	1.2933 (127)	1.25
$G_{2b} \times 10^3$	4.823 (33)	4.790 (31)	4.59
	$v_3 = 1/v_6 = 1$		
G_c	9301.155 (127)	9301.148 (125)	9015.270 (235)
$G_{c,K}$	-6.3011 (259)	-6.3025 (256)	-6.373 (24)
$G_{c,J} \times 10^3$	-45.200 (75)	-45.348 (75)	-43.47
$G_{c,KK} \times 10^3$	16.310 (311)	16.395 (306)	16.02
$G_{c,JK} \times 10^6$	-84.42 (233)	-82.33 (228)	-79.
$G_{c,JJ} \times 10^6$	0.1212 (144)	0.1235 (132)	0.116
$G_{2c} \times 10^3$	14.050 (88)	13.926 (72)	13.12
$G_{2c,K} \times 10^6$	-297.5 (209)	-282.1 (169)	-270.
$G_{2c,J} \times 10^9$	-470.2 (140)	-441.5 (125)	-420.
	$v_2 = 1/v_6 = 1$		
G_c	459.	459.	480.

Notes: Numbers in parentheses are one standard deviation in units of the least significant figures. Parameters values without uncertainties were estimated and kept fixed in the analyses, see Section 5.

Table 5. Vibrational energies E (cm^{-1}) and changes ΔX of spectroscopic parameters (MHz) of $\text{H}_2\text{C}^{34}\text{S}$ in excited vibrational states.

Parameter	$v_4 = 1$	$v_6 = 1$	$v_3 = 1$	$v_2 = 1$
E	990.02140 (11)	990.355	1049.828	1455.391
$\Delta(A - (B + C)/2)$	-142.68	635.42	-223.19	2512.78
$\Delta(B + C)/2$	-3.25192 (173)	-11.25386 (193)	-105.36274 (121)	-26.27430 (115)
$\Delta(B - C)/4$	-4.8659 (50)	12.1687 (49)	-0.98868 (171)	6.71131 (180)
$\Delta D_K \times 10^3$	776.1		-27.0	2053.0
$\Delta D_{JK} \times 10^3$	-5.321	2.48	-2.52	23.66
$\Delta D_J \times 10^6$	184.3	102.5	152.6	-101.6
$\Delta d_1 \times 10^6$	-10.83	-81.3	-19.3	
$\Delta d_2 \times 10^6$		-30.96	-6.04	
$\Delta H_{KJ} \times 10^6$	8.55	8.55		-14.0
$\Delta H_J \times 10^9$		-0.4	1.5	
$\Delta h_1 \times 10^9$		1.33		

Notes: Watson's S reduction was used in the representation I^r . $\Delta X = X_{\text{vib}} - X_0$. Numbers in parentheses are one standard deviation in units of the least significant figures. Parameters values without uncertainties were estimated and kept fixed in the analyses. Empty fields indicate ΔX was not used in the final analysis.

5.2. $\text{H}_2\text{C}^{34}\text{S}$

Having assigned rotational transition of H_2CS in the four lowest excited vibrational states up to fairly high values of K_a we wondered if excited state transitions of $\text{H}_2\text{C}^{34}\text{S}$ and even of H_2^{13}CS are assignable in the OSU spectral recordings. Quantum-chemical calculations were performed for both isotopologues to evaluate vibrational energies and first-order Coriolis coupling parameters $G_i(x, y)$. Improved ground state parameters were already available at that time although not to the extent as in our account on isotopic H_2CS [32]. Vibrational differences ΔX and centrifugal distortion corrections to the $G_i(x, y)$ were evaluated from the best available H_2CS values by scaling with isotopic ratios of appropriate powers of $A - (B + C)/2$, $(B + C)/2$ and $(B - C)/4$ in their ground vibrational states as done for various isotopic species in our previous study [32].

Only some of the strongest $K_a = 0$ transitions in $v_4 = 1$ and $v_6 = 1$ were identified for H_2^{13}CS with some certainty and were not further considered. Quite extensive assignments could be made in the case of $\text{H}_2\text{C}^{34}\text{S}$ with $3 \leq J \leq 11$ and K_a extending to 6, 8, 6 and 5 for $v_4 = 1$, $v_6 = 1$, $v_3 = 1$ and $v_2 = 1$, respectively. Uncertainties of 100 kHz were applied throughout. No attempt was unfortunately made to record transitions of vibrationally excited $\text{H}_2\text{C}^{34}\text{S}$ in Cologne.

We employed results of an MP2/aug-cc-pwCVQZ anharmonic force field calculation, as described in Section 4, to evaluate ground state rotational parameters, their vibrational changes, first-order Coriolis coupling parameters $G_i(x, y)$ and equilibrium quartic and sextic centrifugal distortion parameters of $\text{H}_2\text{C}^{34}\text{S}$. The experimental H_2CS values determined in Section 5.1 were scaled with calculated $\text{H}_2\text{C}^{34}\text{S}/\text{H}_2\text{CS}$ ratios wherever appropriate as was done for isotopic cyclopropanone [67] and included the $G_i(x, y)$. To evaluate the distortion corrections to the $G_i(x, y)$, we scaled each of the H_2CS corrections with $\text{H}_2\text{C}^{34}\text{S}/\text{H}_2\text{CS}$ ratios of the appropriate $G_i(x, y)$ and scaled these values with $\text{H}_2\text{C}^{34}\text{S}/\text{H}_2\text{CS}$ ratios of the appropriate spectroscopic parameters; e.g., we scaled $G_{i,J}(x, y)$ with the ratio of $(B + C)/2$. We searched subsequently for parameters whose fitting would improve the fit as described in Section 4. Besides the obvious choices of $\Delta(B + C)/2$ and $\Delta(B - C)/4$ and some of the interaction parameters it became clear that fitting of one of the vibrational energies was necessary to achieve a satisfactory fit. The best result was obtained by fitting the energy of $v_4 = 1$. The ground state rotational data [32] were included in the final fit and the ground state parameters fitted as in the case of the H_2CS isotopologue. Fitting of further spectroscopic parameters, such as changes in the quartic centrifugal distortion parameters, had only minute effects on the quality of the fit and the resulting uncertainties or the changes in value were usually too large.

The resulting ground state spectroscopic parameters are presented in Table 1 as well, the interaction parameters are given in Table 4 and the vibrational energies and changes ΔX of spectroscopic parameters can be found in Table 5. The excited state data alone were fitted

Table 6. Ground state spectroscopic parameters (MHz) of H₂C₂S from present data set in comparison to values from a high-resolution IR study and from a rotational study.

Parameter	present	previous	
		Ref. [44]	Ref. [43] ^a
$A - (B + C)/2$	280916.1 (227)	280834.764 (78)	281083. (78)
$(B + C)/2$	5601.994368 (127)	5601.993823 (105)	5601.994204 (218)
$(B - C)/4$	28.740720 (18)	28.740742 (17)	28.74086 (32)
D_K	24.6191	24.6191 (30)	24.6191
$D_{JK} \times 10^3$	168.330 (46)	168.330 (26)	168.212 (74)
$D_J \times 10^3$	1.08513 (10)	1.08418 (16)	1.08559 (36)
$d_1 \times 10^6$	-25.426 (34)	-25.470 (33)	-25.55 (63)
$d_2 \times 10^6$	-5.908 (91)	-6.140 (75)	-5.15 (32)
$H_K \times 10^3$	7.387	7.387 (33)	7.387
$H_{KJ} \times 10^6$	-400.0 (44)	-414.4 (21)	-413.5 (70)
$H_{JK} \times 10^9$	617.3 (130)	582.8 (113)	714.7 (184)
$L_{KKJ} \times 10^9$	-866. (144)	-338. (61)	-517. (225)
$L_{JK} \times 10^9$	-2.365 (272)	-2.73 (52)	
$P_{KKJ} \times 10^9$	-52.36 (148)	-58.04 (60)	-54.61 (229)
$P_{KJ} \times 10^9$	-0.109	-0.109 (7)	

Notes: Watson’s S reduction was used in the representation I^r . Numbers in parentheses are one standard deviation in units of the least significant figures. Parameters without uncertainties were taken from Ref. [44] and kept fixed in the analyses. Empty fields indicate parameters not used in the analysis.

^aRefit of Ref. [43], see Section 5.3.

to 81.4 kHz on average, marginally improving to 79.1 kHz after addition of the ground state rotational data.

5.3. Thioketene

A peculiar series of lines in the vicinity of the H₂C³⁴S lines remained unassigned. The appearance in the Loomis–Wood diagrams resembled somewhat those of thioformaldehyde even though it is even closer to the prolate symmetric top limit with a κ of -0.9992 . However, it became evident quite quickly that between two seemingly adjacent lines there were two more lines of similar intensity and regularly spaced. The molecule had to be a heavier one with $(B + C)/2$ nearly one-third of the H₂C³⁴S value. Thioketene was a plausible candidate. The assignment could be established with the help of previous laboratory data [41–43]. The previous data extended to $J = 20 - 19$ up to 226 GHz. We extended the line list from 234 to 361 GHz corresponding to $20 \leq J \leq 32$ with $K_a \leq 7$.

Uncertainties of 20 kHz were assigned to the $J = 3 - 2$ data [41], 10 kHz to a set of $K_a = 1$ Q -branch transitions [42], 15 kHz to the remaining extensive microwave and millimetre wave data [43] and initially 50 kHz to the OSU data which were reduced to 30 kHz in the last fit.

The resulting spectroscopic parameters are provided in Table 6 together with parameters from a far- and mid-IR spectroscopic study [44] which also took into account previous rotational data and those of a refit of the data from Ref. [43]. The refit permits all parameters used in the fits to be compared directly in values and in uncertainties. The rms values are respectively 12.9 kHz [41], 8.9 kHz [42], 15.9 kHz [43] and finally 26.5 kHz for the OSU data.

6. Discussion

An extensive set of spectroscopic parameters of eighth-order plus one decic distortion parameter were required to fit the ground state rotational data of H₂CS shown in Table 1 whereas only parameters up to sixth order were needed in the diagonal part of the Hamiltonian to fit the excited state data of this isotopologue, see Tables 2 and 3. Explanations are certainly that no $\Delta K_a = 0$ Q -branch transitions and no transitions involving $\Delta K_a = 2$ are in the fit for the excited states because these lines are weaker than corresponding ground state transitions by factors of around 100 and more. In addition, the coverage of R -branch transitions is also less

extensive in particular in the Cologne data. Some may question the presence of parameters in the fit such as $\Delta H_{J,6}$. It is not surprising that $F_{j,k}(x,y)$ were not required in the fit because H₂CS is rather close to the prolate symmetric limit and for a symmetric top rotor either $G_i(x,y)$ or $F_{j,k}(x,y)$ may be used to fit a particular Coriolis or related interaction.

The successful fit of essentially all ν_2 transition frequencies [22] at a presumably improved rms and the better fit of the ν_4 , ν_6 and ν_3 data set from Ref. [25] are testament to the importance of including $v_2 = 1$ and its perturbation into the analysis. There are a small number of rotational transitions with relatively large residuals, for example two higher J transitions of $v_3 = 1$ with $K_a = 11$. It is frequently difficult to determine if such residuals at the edge of the data set are a result of missing parameters that cannot be determined yet with enough significance or if the lines have been misjudged. The slight increase from one J to the next leaves room for the first interpretation but is statistically not meaningful.

A comparison of the uncertainties in the excited state parameters of the first combined fit in Table 2 with the ones of the second combined fit in Table 3 is instructive. The uncertainties of parameters with J dependence hardly change for $v_4 = 1$, $v_6 = 1$ and $v_3 = 1$ suggesting their uncertainties are predominantly determined through the rotational data. This is understandable as the rotational data are more accurate and extend to similar or mostly even higher quantum numbers. The larger number of rovibrational transition frequencies moderates this aspect, but only somewhat. The situation is different for the vibrational energies and the purely K -dependent parameters despite the use of one diagonal and one off-diagonal parameter more in the fit. This indicates that their uncertainties are mostly established through the rovibrational data. In the absence of $\Delta K_a = 2$ transitions in the excited states data the rotational data still contribute more indirectly to the purely K -dependent parameters through improving the accuracies of J -dependent parameters and through sampling resonances. The sampling of resonances may also contribute directly to establishing the K -level structure even of a symmetric top rotor if transitions within each state at the resonance are observed along with perturbation mediated transitions between the states as in multiple cases in the excited state spectra of methyl cyanide [55]. The effect of the rovibrational data on the uncertainties in the ground vibrational states in Table 1 is much less pronounced because of $\Delta K_a = 2$ transitions from rotational data [32] and from ground state combination differences extracted from an electronic spectrum [26]. The rovibrational data were also important for $G_a(4,6)$ and its purely K -dependent distortion corrections in Table 4. Remarkable are also some improvements in higher order corrections to $G_c(3,6)$.

We compare next selected spectroscopic parameters from our study with those from other experimental studies and from quantum-chemical calculations. Coriolis or other rotational resonances do not affect vibrational energies. Since the experimental rovibrational spectra access transitions with low J and K_a quantum numbers differences in the fitting should result in minute differences in the vibrational energies at most.

A subset of interaction parameters of H₂CS are compared in Table 7. We discuss the signs of the $G_i(x,y)$ separately as these are usually not determinable from the fits. The $G_a(4,6)$ values all agree well or very well in magnitude. The agreement is also quite good among the two quantum-chemical values of $G_b(3,4)$ and among the present $G_c(3,6)$ and the quantum-chemical values. The agreement is quite different between these experimental $G_i(x,y)$ and our values as well as for the distortion correction as far as they were determined. It is noteworthy that the corrections to $G_a(4,6)$ from the more recent IR study [25] are similar in magnitude to ours but of opposite sign. It is difficult to draw conclusions from this aspect as the agreement is worse for the interaction parameters involving $v_3 = 1$. A plausible explanation for the deviations are perturbations from $v_2 = 1$ which were not taken into account. In fact, $F_{bc}(4,6)$ was introduced in the two early IR studies [23, 24] to account for perturbations of $v_4 = 1$ and $v_6 = 1$ by $v_2 = 1$ as specifically mentioned in the laser Stark study [23]. We introduced parameters into the fit to model interactions of $v_2 = 1$ with $v_4 = 1$ and $v_6 = 1$, so the absence of $F_{bc}(4,6)$ in our fit does not argue against that proposition. One of the early IR studies [24] employed also distortion corrections to $G_a(4,6)$ of which $G_{a,K}(4,6)$ agrees well whereas there are factors of a few in the other two cases.

Table 7. Selected interaction parameters (MHz) of H₂CS from from the second combined fit of this work (TW) in comparison to values from previous experimental works and to values from quantum-chemical calculations (QC).

Parameter	Experimental				QC	
	TW	Ref. [25] ^a	Ref. [24]	Ref. [23]	CC ^b	MP2 ^c
$G_a(4, 6) \times 10^{-3}$	-300.2114	-300.37	300.228	299.918	299.33	299.67
$F_{bc}(4, 6)$			58.	49.		
$G_{a,K}(4, 6)$	58.37	-77.7	-56.0			
$G_{a,J}(4, 6)$	0.86719	-0.55	-2.6			
$G_{2a}(4, 6)$	-0.416		2.			
$G_b(3, 4) \times 10^{-3}$	-2.177 ^d	4.55	4.9	1.6	-2.44	-2.18
$G_{b,K}(3, 4)$		45.				
$G_{b,J}(3, 4) \times 10^3$	-97.86	114.				
$G_c(3, 6) \times 10^{-3}$	9.3012	2.30	12.2	9.2	8.73	8.93
$G_{c,K}(3, 6)$	-6.30	-16.				
$G_{c,J}(3, 6) \times 10^3$	-45.20	-343.				

Notes: The last digit of each value is uncertain. Empty fields indicate values not determined. The signs of the $G_i(x, y)$ are usually not determinable in the fits but matter for the IR intensities in the present case, see also Section 5.1.

^aA value of ~ 0.004 kHz was also determined for $G_{a,JJ}(4, 6)$.

^bCoupled cluster calculation CCSD(T)/cc-pVTZ from Ref. [27].

^cMP2/aug-cc-pwCVQZ from this work, see Section 4.

^dKept fixed in the analysis, see Section 5.1.

Table 8. Selected low order ΔX_i parameters (MHz) of H₂CS from from the second combined fit of this work (TW) in comparison to values from previous experimental works and to values from quantum-chemical calculations (QC).

Parameter	Experimental				QC	
	TW	Ref. [25]	Ref. [22]	Ref. [24]	Ref. [23]	CC ^a
$\Delta A_4 \times 10^{-3}$	-0.1457	3.65			-2.17	-4.143
ΔB_4	-13.281	-71.0		-68.	-155.	-73.
ΔC_4	6.884	5.6		15.	32.	4.
$\Delta D_{K,4}$	0.772	-0.9			^b	
$\Delta A_6 \times 10^{-3}$	0.6237	-3.18			2.43	4.817
ΔB_6	13.966	18.3		-87.	-84.	12.
ΔC_6	-36.11	-75.7		91.	159.	-40.
$\Delta D_{K,6}$		1.7			^b	
$\Delta(A_4 + A_6) \times 10^{-3}$	0.4779	0.479		0.228	0.17	0.574
$\Delta D_{K,4} + \Delta D_{K,6}$	0.772	0.73			^b	
$\Delta A_3 \times 10^{-3}$	-0.3110	-0.330		-0.329	-0.329	-0.332
ΔB_3	-110.0383	-115.		-120.	-84.	-109.
ΔC_3	-106.074	-69.7		-140.	-102.	-102.
$\Delta D_{K,3}$	0.027	0.2			^b	
$\Delta A_2 \times 10^{-3}$	2.4831		2.4763			2.898
ΔB_2	-13.1150		54.31			46.
ΔC_2	-40.9393		-39.49			-41.
$\Delta D_{K,2}$	2.041		1.8			

Notes: The last digit of each value is uncertain, except for ΔB_3 and ΔC_3 from Ref. [24] where it is one digit earlier. Empty fields indicate usually values not determined. Please note that some studies [23, 25] employed the A reduction only but differences are small with respect to the uncertainties and the quoted digits.

^aCoupled cluster calculation CCSD(T)/cc-pVTZ from Ref. [27].

^b ΔK values are given, but are very uncertain.

The early IR studies [23, 24] did not address the signs of the $G_i(x, y)$. The later IR study [25] presents $G_a(4, 6)$ as negative and $G_b(3, 4)$ as well as $G_c(3, 6)$ as positive. But it is not clear if the signs from that work can be compared directly because only the operator associated with $G_c(3, 6)$ was defined as imaginary whereas all $G_i(x, y)$ operators are commonly defined as imaginary. With $G_a(4, 6)$ being negative it was necessary in our fits that the signs of $G_b(3, 4)$ and $G_c(3, 6)$ differ. The P -branch of ν_2 was calculated to be stronger than the R -branch in Ref. [31], in accordance with our interpretation of Fig. 1 of Ref. [22], but in contrast to Ref. [34].

Some low order ΔX_i parameters of H₂CS are shown for comparison purpose in Table 8. The agreement is often quite poor for the experimental $v_4 = 1$ and $v_6 = 1$ parameters. This can be attributed to the a -type Coriolis resonance, its treatment and the data coverage in the case of ΔA and ΔD_K . Their sums $\Delta A_4 + \Delta A_6$ and $\Delta D_{K,4} + \Delta D_{K,6}$ are better constrained and agree much better. The agreement is very good and good for these values from Ref. [25] even though the individual parameters differ very much. The sum $\Delta A_4 + \Delta A_6$ was only determined in Ref. [24]. This is an indication of the importance of the rotational data from this study for constraining the spectroscopic parameters. And the uncertainty of $\Delta A_4 + \Delta A_6$ is even in the present study with 119 kHz much smaller than that of $\Delta A_4 - \Delta A_6$ with 472 kHz. Correlations with other parameters may complicate the situation in particular for previous studies; constraints in the present study, including the omission of some parameter differences, have helped to reduce correlation.

The $v_3 = 1$ ΔX_i from Refs. [23, 24] agree reasonably well with the present values if we take into account the very small ν_3 data set in both studies. Therefore, we attribute the disagreement of the $v_4 = 1$ and $v_6 = 1$ values of ΔB and ΔC in these studies to the use of $F_{bc}(4, 6)$ in their fits. The disagreement of ΔC_3 and ΔC_6 from Ref. [25] with our values is connected with the very different $G_c(3, 6)$ value.

The ΔX_2 from Ref. [22] agree quite well with ours except for ΔB_2 which is clearly a consequence of neglecting the distant but strong Coriolis interaction with $v_4 = 1$. This is fairly well mirrored in the deviation of ΔB_4 from Ref. [25] and even better mirrored in the ΔB_4 and ΔB_2 values from a quantum-chemical study [27]. It is necessary to mention that quantum-chemical force field calculations usually do not determine resonance effects on spectroscopic parameters except possibly for the impact of Fermi or other anharmonic resonances on the vibrational energies. Moreover, quantum-chemical calculations provide commonly first-order vibrational corrections $\alpha_j^{B^i}$ associated with the i -axis rotational parameter and the vibration ω_j and not the ΔX_j^i . The first-order vibrational corrections $\alpha_j^{B^i}$ are defined via

$$B_v^i = B_e^i - \sum_j \alpha_j^{B^i} (v_j + \frac{1}{2}) + \sum_{j \leq k} \gamma_{jk}^{B^i} (v_j + \frac{1}{2})(v_k + \frac{1}{2}) + \dots$$

where B_e^i is the equilibrium rotational parameter associated with the i -axis, B_v^i is the rotational parameter in an excited state v , v_j and v_k are the excitation quanta of ν_j and ν_k in this state v and the $\gamma_{jk}^{B^i}$ are second-order vibrational corrections; higher order corrections may be defined equivalently. The equation $\Delta X_j^i = -\alpha_j^{B^i}/2$ is commonly assumed but holds only strictly if the $\gamma_{jk}^{B^i}$ and so on were zero. The ΔX_j^i taken from a quantum-chemical calculation [27] agree well to reasonably well if the values are not or not strongly affected by resonances. These include ΔC_4 , ΔB_6 , ΔB_3 , ΔC_2 and to a lesser extend $\Delta A_4 + \Delta A_6$, ΔA_3 and ΔA_2 . The deviations are also quite small for ΔC_6 and ΔC_3 but would probably agree even better with our values if the effect of $G_c(3, 6)$ is taken into account.

We have inspected calculated transition frequencies of H₂CS [34] derived from a quantum-chemically calculated potential energy surface that was refined taking evaluated experimental data [33] into account. We inspected $J = 3 - 2$ transition frequencies of the five lowest vibrational states and compared these with values derived from our second combined analysis. The agreements were good (deviations much less than 100 kHz) to reasonable (exceeding about 1 MHz). The largest deviations for these low- J transitions were ~ 1.0 MHz in $v_4 = 1$ and $v_6 = 1$,

about 1.6 MHz in $v = 0$, ~ 2.0 MHz in $v_3 = 1$ and almost 4 MHz in $v_2 = 1$. Further refinement may be possible taking our present H₂CS transition frequencies into account.

The data of H₂C³⁴S in excited vibrational states could be fitted well with varying only a relatively small number of spectroscopic parameters in Table 5. Unsurprisingly, these involved changes associated with B and C and a rather small number of interaction parameters, see Table 4. The change in $\Delta(B + C)/2$ from the initial values is ~ 0.1 MHz for $v_4 = 1$ up to ~ 0.9 MHz for $v_6 = 1$. The change in $\Delta(B - C)/4$ is ~ 0.07 MHz in the case of $v_6 = 1$ and much smaller otherwise. It is difficult to evaluate how different the $\Delta(A - (B + C)/2)$ may be; deviations of some megahertz cannot be ruled out. No corrections to quartic distortion parameters needed to be released which indicates the quality of the applied scaling procedure [67]. The determination of one vibrational energy ($v_4 = 1$) through the Coriolis perturbations in the spectrum improved the quality of the fit substantially. The change from the initial estimate of 990.017 cm^{-1} is very small but should be viewed with some caution nevertheless because its value will depend somewhat on the exact energies of the remaining states and on the exact values of the $\Delta(A - (B + C)/2)$. Improvements in the ground state spectroscopic parameters of H₂C³⁴S in Table 1 with respect to earlier values [32] should also be viewed with caution in particular for the purely K -dependent parameters. The application of realistic uncertainties of the $\Delta(A - (B + C)/2)$ may eliminate these improvements. The assigned uncertainties of 100 kHz to the experimental transition frequencies are quite appropriate at an rms of ~ 80 kHz.

The additional transition frequencies of H₂C₂S lead to improvements in the spectroscopic parameters that are between slight and substantial with respect to the previous rotational study [43]. The change in values of $A - (B + C)/2$ and d_2 may be connected but may also be a result of the two more spectroscopic parameters of which one was kept fixed in the analysis. The comparison is less favourable with respect to values from Ref. [44] where D_K and H_K were fitted and still most parameters display somewhat smaller uncertainties. Our L_{JK} value has a smaller uncertainty but that is merely a consequence of fixing P_{KJ} in our fit because it was not determinable with sufficient significance. A combined fit of our new data with those employed in Ref. [44] could result in a further improvement of the thioketene ground state parameters.

It is possible that transitions of thioketene with $K_a = 8$ or 9 are present in our OSU recordings but it would be very difficult to locate them as $v = 0$ is perturbed by $v_9 = 1$ and $v_9 = 1$ is part of a massive resonance system [44]. The $v = 0$ energy of $K_a = 11$ is below $K_a = 10$ of $v_9 = 1$ whereas it is calculated to be opposite for the next higher values of K_a . Another detail not discussed in that work is that $K_a = 7$ of $v = 0$ is very close to $K_a = 4$ of $v_9 = 1$ which may not matter for data recorded with IR accuracy but may well affect the rotational data obtained with microwave accuracy. We mention also that Ref. [44] presented a combined analysis of $v = 0$, $v_9 = 1$ and $v_6 = 1$ in which the perturbation of $v = 0$ by $v_9 = 1$ was taken into account.

7. Conclusion

We have presented assignments of rotational transitions pertaining to H₂CS and H₂C³⁴S in their lowest four excited vibrational states along with analyses of their intricate Coriolis perturbations. Sets of IR data were employed in the case of the main isotopologue. The results highlight the importance of taking resonances with $v_2 = 1$ into account in the analyses of the three lowest fundamental states of the main isotopologue which has been carried out here for the first time. Not only was it possible to fit essentially all ν_2 data well, in contrast to the initial study [22], but also to achieve a better fit of an extensive set of ν_4 , ν_6 and ν_3 data [25].

Deriving starting spectroscopic parameters from the main isotopologue permitted to fit H₂C³⁴S rotational data well with varying only a small subset of the parameters.

We have extended the set of rotational transition frequencies of thioketene to higher values of J thus improving the spectroscopic parameters considerably with respect to the latest millimetre wave investigation [43].

Acknowledgement(s)

We thank Don McNaughton for sending us the ν_2 data of H₂CS and Jean-Marie Flaud for providing the 10 μ m line list prior to publication and the spectrum of H₂CS in a digital form more recently. We are grateful to Frank C. De Lucia for making equipment available to carry out the measurements at The Ohio State University and the late Manfred Winnewisser for assistance during these measurements. We thank Christian P. Endres and Monika Koerber for support during some of the measurements in Köln. We thank the Regionales Rechenzentrum der Universität zu Köln (RRZK) for providing computing time on the DFG funded High Performance Computing System CHEOPS. Our research benefited from NASA’s Astrophysics Data System (ADS).

Disclosure statement

No potential conflict of interest was reported by the author(s).

Data availability statement

The line, parameter and fit files with information on the setup of the parameter file, the transition frequencies with uncertainties, quantum numbers and residuals between observed frequencies and those calculated from the spectroscopic parameters, the parameters with codes, values and uncertainties and finally the correlation coefficients are available as supplementary material to this article together with an explanatory file. These files are all regular text files.

These and auxiliary files are also available in the Cologne Database for Molecular Spectroscopy (CDMS) [68, 69] at <https://cdms.astro.uni-koeln.de/classic/predictions/daten/H2CS/2023/>. Calculations of the rotational spectra are available in the catalogue section of the CDMS at <https://cdms.astro.uni-koeln.de/classic/entries/>.

Funding

We acknowledge support by the Deutsche Forschungsgemeinschaft via the collaborative research centers SFB 494 project E2 and SFB 956 (project ID 184018867) project B3 as well as the Gerätezentrum SCHL 341/15-1 (“Cologne Center for Terahertz Spectroscopy”). We are grateful to NASA for its support of the OSU program in laboratory astrophysics and the ARO for its support of the study of large molecules.

References

- [1] M.W. Sinclair, N. Fourikis, J.C. Ribes, B.J. Robinson, R.D. Brown and P.D. Godfrey, *Aust. J. Phys.* **26**, 85 (1973).
- [2] W.M. Irvine, P. Friberg, N. Kaifu, K. Kawaguchi, Y. Kitamura, H.E. Matthews, Y. Minh, S. Saito, N. Ukita and S. Yamamoto, *Astrophys. J.* **342**, 871 (1989).
- [3] M. Agúndez, J.P. Fonfría, J. Cernicharo, J.R. Pardo and M. Guélin, *Astron. Astrophys.* **479** (2), 493–501 (2008).
- [4] A. Heikkilä, L.E.B. Johansson and H. Olofsson, *Astron. Astrophys.* **344**, 817–847 (1999).
- [5] S. Martín, J. Martín-Pintado, R. Mauersberger, C. Henkel and S. García-Burillo, *Astrophys. J.* **620** (1), 210–216 (2005).
- [6] S. Muller, A. Beelen, M. Guélin, S. Aalto, J.H. Black, F. Combes, S.J. Curran, P. Theule and S.N. Longmore, *Astron. Astrophys.* **535**, A103 (2011).

- [7] L.M. Woodney, M.F. A’Hearn, J. McMullin and N. Samarasinha, *Earth Moon and Planets* **78**, 69–70 (1997).
- [8] F.F. Gardner, B. Hoglund, C. Shukre, A.A. Stark and T.L. Wilson, *Astron. Astrophys.* **146**, 303–306 (1985).
- [9] S.E. Cummins, R.A. Linke and P. Thaddeus, *Astrophys. J. Suppl. Ser.* **60**, 819 (1986).
- [10] H. Minowa, M. Satake, T. Hirota, S. Yamamoto, M. Ohishi and N. Kaifu, *Astrophys. J. Lett.* **491** (1), L63–L66 (1997).
- [11] N. Marcelino, J. Cernicharo, E. Roueff, M. Gerin and R. Mauersberger, *Astrophys. J.* **620** (1), 308–320 (2005).
- [12] M.L.R. van ’t Hoff, E.F. van Dishoeck, J.K. Jørgensen and H. Calcutt, *Astron. Astrophys.* **633**, A7 (2020).
- [13] Y. Oya and S. Yamamoto, *Astrophys. J.* **904** (2), 185 (2020).
- [14] S. Spezzano, O. Sipilä, P. Caselli, S.S. Jensen, S. Czakli, L. Bizzocchi, J. Chantzos, G. Esplugues, A. Fuente and F. Eisenhauer, *Astron. Astrophys.* **661**, A111 (2022).
- [15] D.R. Johnson and F.X. Powell, *Science* **169** (3946), 679–680 (1970).
- [16] D.R. Johnson, F.X. Powell and W.H. Kirchhoff, *J. Mol. Spectrosc.* **39**, 136–145 (1971).
- [17] Y. Beers, G.P. Klein, W.H. Kirchhoff and D.R. Johnson, *J. Mol. Spectrosc.* **44** (3), 553–557 (1972).
- [18] A.P. Cox, S.D. Hubbard and H. Kato, *J. Mol. Spectrosc.* **93** (1), 196–208 (1982).
- [19] R.D. Brown, P.D. Godfrey, D. McNaughton and K. Yamanouchi, *Mol. Phys.* **62** (6), 1429–1433 (1987).
- [20] B. Fabricant, D. Krieger and J.S. Muentner, *J. Chem. Phys.* **67** (4), 1576–1586 (1977).
- [21] J.W.C. Johns and W.B. Olson, *J. Mol. Spectrosc.* **39** (3), 479–505 (1971).
- [22] D. McNaughton and D.N. Bruget, *J. Mol. Spectrosc.* **159** (2), 340–349 (1993).
- [23] D.J. Bedwell and G. Duxbury, *J. Mol. Spectrosc.* **84** (2), 531–558 (1980).
- [24] P.H. Turner, L. Halonen and I.M. Mills, *J. Mol. Spectrosc.* **88** (2), 402–419 (1981).
- [25] J.M. Flaud, W.J. Lafferty, A. Perrin, Y.S. Kim, H. Beckers and H. Willner, *J. Quant. Spectrosc. Radiat. Transfer* **109**, 995–1003 (2008).
- [26] D.J. Clouthier, G. Huang, A.G. Adam and A.J. Merer, *J. Chem. Phys.* **101** (9), 7300–7310 (1994).
- [27] J.M.L. Martin, J.P. Francois and R. Gijbels, *J. Mol. Spectrosc.* **168** (2), 363–373 (1994).
- [28] S. Carter and N.C. Handy, *J. Mol. Spectrosc.* **192** (2), 263–267 (1998).
- [29] H.D. Meyer, F.L. Quéré, C. Léonard and F. Gatti, *Chem. Phys.* **329** (1-3), 179–192 (2006).
- [30] A. Yachmenev, S.N. Yurchenko, T. Ribeyre and W. Thiel, *J. Chem. Phys.* **135** (7), 074302–074314 (2011).
- [31] A. Yachmenev, I. Polyak and W. Thiel, *J. Chem. Phys.* **139** (20), 204308–204308 (2013).
- [32] H.S.P. Müller, A. Maeda, S. Thorwirth, F. Lewen, S. Schlemmer, I.R. Medvedev, M. Winnewisser, F.C. De Lucia and E. Herbst, *Astron. Astrophys.* **621**, A143 (2019).
- [33] T.M. Mellor, A. Owens, J. Tennyson and S.N. Yurchenko, *J. Mol. Spectrosc.* **391**, 111732 (2023).
- [34] T. Mellor, A. Owens, J. Tennyson and S.N. Yurchenko, *Mon. Not. R. Astron. Soc.* **520** (2), 1997–2008 (2023).
- [35] C. Ochsenfeld, R.I. Kaiser, Y.T. Lee and M. Head-Gordon, *J. Chem. Phys.* **110** (20), 9982–9988 (1999).
- [36] N. Inostroza-Pino, C.Z. Palmer, T.J. Lee and R.C. Fortenberry, *J. Mol. Spectrosc.* **369**, 111273 (2020).
- [37] S. Carter, A.R. Sharma, J.M. Bowman, P. Rosmus and R. Tarroni, *J. Chem. Phys.* **131** (22), 224106–224106 (2009).
- [38] S. Erfort, M. Tschöpe and G. Rauhut, *J. Chem. Phys.* **152** (24), 244104 (2020).
- [39] D.F. Dinu, M. Tschöpe, B. Schröder, K.R. Liedl and G. Rauhut, *J. Chem. Phys.* **157** (15), 154107 (2022).
- [40] A. Maeda, I.R. Medvedev, M. Winnewisser, F.C. De Lucia, E. Herbst, H.S.P. Müller, M. Koerber, C.P. Endres and S. Schlemmer, *Astrophys. J. Suppl. Ser.* **176** (2), 543–550 (2008).
- [41] K. Georgiou, H.W. Kroto and B.M. Landsberg, *J. Mol. Spectrosc.* **77** (3), 365–373 (1979).
- [42] B. Bak, O.J. Nielsen, H. Svanholt, A. Holm, N.H. Toubro, A. Krantz and J. Laurenzi, *Acta Chem. Scand. A* **33** (2), 161–165 (1979).
- [43] M. Winnewisser and E. Schaefer, *Z. Naturforsch. A* **35**, 483–489 (1980).
- [44] D. McNaughton, E.G. Robertson and L.D. Hatherley, *J. Mol. Spectrosc.* **175** (2), 377–385 (1996).
- [45] J. Cernicharo, C. Cabezas, M. Agúndez, B. Tercero, J.R. Pardo, N. Marcelino, J.D. Gallego, F. Tercero, J.A. López-Pérez and P. de Vicente, *Astron. Astrophys.* **648**, L3 (2021).
- [46] D.T. Petkie, T.M. Goyette, R.P.A. Bettens, S.P. Belov, S. Albert, P. Helminger and F.C. De Lucia,

- Rev. Sci. Instrum. **68** (4), 1675–1683 (1997).
- [47] I. Medvedev, M. Winnewisser, F.C. De Lucia, E. Herbst, E. Białkowska-Jaworska, L. Pszczółkowski and Z. Kisiel, *J. Mol. Spectrosc.* **228** (2), 314–328 (2004).
- [48] F.C. De Lucia, *J. Mol. Spectrosc.* **261** (1), 1–17 (2010).
- [49] G. Winnewisser, A.F. Krupnov, M.Y. Tretyakov, M. Liedtke, F. Lewen, A.H. Saleck, R. Schieder, A.P. Shkaev and S.V. Volokhov, *J. Mol. Spectrosc.* **165** (1), 294–300 (1994).
- [50] G. Winnewisser, *Vib. Spectrosc.* **8** (2), 241–253 (1995).
- [51] L.H. Xu, R.M. Lees, G.T. Crabbe, J.A. Myshrall, H.S.P. Müller, C.P. Endres, O. Baum, F. Lewen, S. Schlemmer, K.M. Menten and B.E. Billinghurst, *J. Chem. Phys.* **137** (10), 104313 (2012).
- [52] H.S.P. Müller and S. Brünken, *J. Mol. Spectrosc.* **232** (2), 213–222 (2005).
- [53] A. Maeda, F.C. De Lucia, E. Herbst, J.C. Pearson, J. Riccobono, E. Trosell and R.K. Bohn, *Astrophys. J. Suppl. Ser.* **162** (2), 428–435 (2006).
- [54] P. Groner, M. Winnewisser, I.R. Medvedev, F.C. De Lucia, E. Herbst and K.V.L.N. Sastry, *Astrophys. J. Suppl. Ser.* **169** (1), 28–36 (2007).
- [55] H.S.P. Müller, A. Belloche, F. Lewen, B.J. Drouin, K. Sung, R.T. Garrod and K.M. Menten, *J. Mol. Spectrosc.* **378**, 111449 (2021).
- [56] H.S.P. Müller, J.C. Guillemin, F. Lewen and S. Schlemmer, *J. Mol. Spectrosc.* **384**, 111584 (2022).
- [57] I.R. Medvedev, M. Winnewisser, B.P. Winnewisser, F.C. De Lucia and E. Herbst, *J. Mol. Struct.* **742** (1-3), 229–236 (2005).
- [58] H.M. Pickett, *J. Mol. Spectrosc.* **148** (2), 371–377 (1991).
- [59] A.M. Tolonen, M. Koivusaari, R. Paso, J. Schroderus, S. Alanko and R. Anttila, *J. Mol. Spectrosc.* **160** (2), 554–565 (1993).
- [60] T. Tanaka and Y. Morino, *J. Mol. Spectrosc.* **33** (3), 538–551 (1970).
- [61] H.S.P. Müller, E.A. Cohen and D. Christen, *J. Mol. Spectrosc.* **216** (2), 335–344 (2002).
- [62] O.N. Ulenikov, G.A. Onopenko, O.V. Gromova, E.S. Bekhtereva and V.M. Horneman, *J. Quant. Spectrosc. Radiat. Transfer* **130**, 220–232 (2013).
- [63] C. Møller and M.S. Plesset, *Phys. Rev.* **46** (7), 618–622 (1934).
- [64] T.H. Dunning, Jr., *J. Chem. Phys.* **90** (2), 1007–1023 (1989).
- [65] K.A. Peterson and T.H. Dunning, *J. Chem. Phys.* **117** (23), 10548–10560 (2002).
- [66] M.J. Frisch, G.W. Trucks, H.B. Schlegel, G.E. Scuseria, M.A. Robb, J.R. Cheeseman, G. Scalmani, V. Barone, G.A. Petersson, H. Nakatsuji and et al. 2019, Gaussian 16, Revision C.01, Gaussian, Inc., Wallingford CT.
- [67] H.S.P. Müller, A. Brahmi M., J.C. Guillemin, F. Lewen and S. Schlemmer, *Astron. Astrophys.* **647**, A179 (2021).
- [68] H.S.P. Müller, F. Schlöder, J. Stutzki and G. Winnewisser, *J. Mol. Struct.* **742** (1-3), 215–227 (2005).
- [69] C.P. Endres, S. Schlemmer, P. Schilke, J. Stutzki and H.S.P. Müller, *J. Mol. Spectrosc.* **327**, 95–104 (2016).